
Integrated Predictive Artificial Neural Network Fatigue Endurance Limit Model for Asphalt Concrete Pavements

Journal:	<i>Canadian Journal of Civil Engineering</i>
Manuscript ID	cjce-2018-0051.R1
Manuscript Type:	Article
Date Submitted by the Author:	23-Jun-2018
Complete List of Authors:	Isied, Mayzan; University of Texas at Tyler, Civil Engineering Souliman, Mena; University of Texas at Tyler, Department of Civil Engineering
Is the invited manuscript for consideration in a Special Issue? :	Not applicable (regular submission)
Keyword:	Endurance limit, healing, fatigue, artificial neural network, rest period

1 **Integrated Predictive Artificial Neural Network Fatigue Endurance Limit Model for**
2 **Asphalt Concrete Pavements**

3
4 **By**

5
6 **Mayzan M. Isied**

7 Graduate Research Assistant
8 The University of Texas at Tyler
9 Department of Civil Engineering
10 3900 University Blvd, RBS 1028
11 Tyler, TX 75701

12 Telephone: 903-944-6782

13 E-mail: misied@uttyler.edu

14
15 **Mena I. Souliman, Ph.D.**

16 Assistant Professor
17 The University of Texas at Tyler
18 Department of Civil Engineering
19 3900 University Blvd, RBS 1008
20 Tyler, TX 75701

21 Telephone: 903-565-5892

22 E-mail: msouliman@uttyler.edu

23
24

Abstract

Asphalt endurance limit is a strain value if experienced by asphalt pavement layer, no accumulated damage will occur and is directly related to asphalt healing. Therefore, if the pavement experiences this value of strain, or lower, no fatigue damage would accumulate within that pavement section. Beam fatigue test data conducted under the NCHRP Project 9-44A were extracted and utilized to create an Artificial Neural Network predictive model (ANN) to determine the endurance limit strain values for conventional asphalt concrete pavements. The developed ANN model architecture as well as how to utilize it to predict the endurance limit were demonstrated and discussed in detail. Also, a stand-alone equation that is capable in the prediction of the endurance limit strain value, separate from the ANN model environment, was derived utilizing the eclectic extraction approach. The model training and validation data included 934 beam fatigue laboratory data points, as extracted from NCHRP Project 9-44A report. The developed model was able to determine the endurance limit strain value as a function of the stiffness ratio, number of cycles to failure, initial stiffness and rest period, and had a reasonable coefficient of determination (R^2) value, which indicates the reliability of both the developed ANN model and the stand-alone equation. Furthermore, a correlation between the endurance limit strain values, as predicted utilizing the generated regression model under the NCHRP project 944-A, and the endurance limit strain values predicted utilizing the stand-alone ANN derived equation was found with a high coefficient of determination (R^2) value.

44

Keywords: Endurance limit, healing, fatigue, artificial neural network, rest period.

46

47

48

49

50

51

52 1. Introduction

53 Fatigue cracking is one of the major challenges in the flexible pavement design. Fatigue cracking
54 is defined as the longitudinal or interconnect cracks that propagates from the bottom to the top of
55 the asphalt layers under repeated traffic loading cycles. Those cracks usually appear in the outer
56 wheel path for thin Hot Mix Asphalt (HMA) layer and in the inner wheel path for the thick HMA
57 layers (Abojaradeh 2003). The endurance limit is a strain value, below which no accumulated
58 damage will occur to the pavement. Thus, a pavement with a design strain value at the bottom of
59 the HMA layer that is equal to or lower than the endurance limit will never experience fatigue
60 cracking, which classifies it as perpetual pavement (Newcomb 2001). Therefore, the endurance
61 limit is directly related to asphalt healing. Asphalt healing is the ability of the HMA layer to
62 regain its structural initial condition before the loading damage if given enough rest period time
63 between two consecutive loading cycles (Peterson 1984).

64 Current mechanistic design approach assumes that there is an amount of damage
65 associated to each loading cycle the HMA layer is subjected to, and that accumulated damage is
66 consuming a portion of the total fatigue life of the pavement section. However, recent studies
67 demonstrated that a well-constructed pavement section will not experience a fatigue cracking even
68 if it was subjected to large numbers of loading cycles (Willis and Timm 2009; Thompson and
69 Carpenter 2006; Prowell et al. 2010). The above statement drives the need to have a reliable
70 prediction model for the endurance limit values for pavement design process consideration.

71 Growing number of researchers are utilizing the Artificial Neural Network (ANN) as a
72 data mining approach due to its high classification and prediction accuracy. ANN is utilized to
73 solve variety of problems such as pattern classification and function approximation (Setiono et

74 al. 2002). Therefore, ANN modeling was utilized to create the endurance limit prediction model
75 in this research paper.

76 **2. Objective**

77 The study aims to provide a reliable ANN model that has the ability to predict the fatigue
78 endurance limit. To achieve the goal, the previously conducted beam fatigue tests under project
79 NCHRP 944-A were utilized to create the desired model, which classifies strain value as the
80 dependent variable, while the rest period, initial stiffness, number of cycles to failure, and the
81 stiffness ratio are defined as the independent variables. The model was statistically validated and
82 evaluated. Also, a stand-alone correlation equation was extracted via the eclectic extraction
83 approach to be utilized outside the model environment.

84 **3. Literature Review**

85 **3.1 Rest Period and Healing of HMA**

86 Rest period is defined as the time between two consecutive loading cycles. The amount of the
87 damage associated with testing during a rest period is lower than the amount of damage related
88 to the continuous testing due to the healing that occurred during the rest period (Souliman
89 2012).

90 McElvane and Pell (1973) had conducted a research study utilizing the rotating bending
91 fatigue testing technique. The testing was conducted utilizing multi-level loading and random
92 duration of rest periods. The improvement occurred to the fatigue life was not quantified.
93 However, it was concluded that the rest period will improve the fatigue life of the tested
94 specimen.

95 Castro et al (2006) conducted a research study to examine the effect of the rest period on
96 the fatigue life, which concluded that the introduction of 1-second rest period between two .1-

97 second loading times will increase the fatigue life of the tested specimen 10 times. This was
98 completed in comparison to a test result of a specimen that was tested without a rest period.

99 The material self-recovery to its initial status and properties if given enough time to rest
100 is defined as healing. This phenomenon was examined in the literature for many years and
101 various engineering materials (metallic and nonmetallic) were found to have this ability (Suresh
102 1998; Souliman 2012).

103 The three-major mechanisms that prevent the growth of fatigue cracking and induce the
104 crack healing for the non-metallic material such as cement concrete, asphalt concrete, and
105 polymers can be summarized as follows: 1) Crack deflection, 2) Crack-bridging or trapping, and
106 3) Crack-shielding due to micro cracking or phase transformations (Suresh 1998).

107 Lytton (2000) has conducted a research study to evaluate the effect of the healing on the
108 fatigue life and to explain the fracture and healing mechanisms. The fracture-healing
109 mechanisms for the asphalt concrete were classified under two main categories, the surface
110 energy storage and the surface energy release. It was concluded that the surface energy depends
111 mainly on the chemical composition of the binder, while also concluding that the energy balance
112 between the stored and released energy controls the fracture and healing mechanism of the
113 asphalt aggregate mixture.

114 **3.2 HMA Endurance Limit**

115 Wöhler (1860) first introduced the concept of endurance limit in the literature for the metallic
116 materials by the generation of the classical S/N curves. His findings also presented the fact that
117 there is a load level below which the number of cycles to failure will remain constant and will
118 not increase by decreasing the load. This load was defined as the Fatigue Endurance Limit
119 (FEL) for metallic materials.

120 Although the endurance limit concept has been extensively addressed and examined for
121 metallic and other materials, less work was done to study and understand this concept in
122 viscoelastic material, such as asphalt (Souliman 2012).

123 Monismith and McLean (1972) had observed that the relationship between the strain and
124 the loading cycles had converged at approximately 70 micro strains when the loading cycles
125 were around 5 million cycles. Thus, a 70-micro strain was proposed by them as the endurance
126 limit value for the asphalt pavements. Also, Maupin and Freeman (1976) had arrived to the same
127 results and found that the 70-micro strain is the endurance limit for the asphalt pavements.

128 Carpenter (2006) demonstrated in his study that there is an endurance limit for the asphalt
129 pavements and concluded that the endurance limit is dependent on the binder type and its values
130 are limited between 70 to 100-micro strains in some cases. The drawn conclusion by this study
131 matched the previous studies' conclusions in terms of endurance limits values.

132 **3.3 HMA Endurance Limit and Healing Concepts Developed Under NCHRP Project 944A**

133 Souliman (2012) has developed a mathematical procedure to determine the value of the
134 endurance limit based on the asphalt healing under the NCHRP project 944A. The asphalt
135 healing index was defined as the difference in the stiffness ratio between the tests done with rest
136 period and without rest period at the number of cycles to failure for test without rest period as
137 shown in Figure 1.

138 A general stiffness ratio model was generated and utilized to determine the healing index
139 values at different test combinations. The relationship between the healing index and the stiffness
140 ratio at different temperatures is shown in Figure 2. From the endurance limit definition, it is
141 clear that this limit occurs when no damage accumulation occurs in the pavement. Thus, it was
142 defined as the strain value at the value of 0.5 HI. The value of 0.5 HI is equivalent to 0.5 stiffness

143 ratio for tests without rest period, and 1 stiffness ratio for tests with rest period. Three different
144 generations of SR prediction models were developed under this project. The third-generation
145 model was utilized to predict the endurance limit by substituting a stiffness ratio value of 1 (no
146 damage) and a number of cycles to failure of 20,000.

147 It was concluded by this project that the endurance limit is a function of the mixture
148 initial stiffness (referring to the binder type, binder content, air voids, and mix temperature), rest
149 periods between different loading cycles, stiffness ratio, and the number of loading cycles to
150 failure. Furthermore, and due to the endurance limit being a function of all the previous
151 variables, it was stated that there is no single value that represents the endurance limit. The
152 developed models estimated the endurance limit values in a range of 22 to 223-micro strains.

153 **4. The Design of the Experimental Study Done Under Project NCHRP 944-A**

154
155 A factorial experiment was designed to study the effect of six factors on the endurance limit of
156 the asphalt concrete: 1) Binder type, 2) Binder content, 3) Air voids, 4) N_f for a stress-controlled
157 tests 5) Temperature, and 6) Rest periods.

158 The experiment conditions were as follows:

- 159 • Binder types: PG 58-28, PG 64-22, and PG 76-16.
- 160 • Binder content: optimum +5% and optimum - 5%.
- 161 • Air voids: 4.5% and 9.5%.
- 162 • N_f for a strain-controlled test: 2 levels L and H.
- 163 • Temperature: 40, 70, and 100 °F.
- 164 • Rest period: 0 and 5 sec.

165 The full factorial design, if used, would results in a total of 432 tests (3 binder types x 2
166 binder content x 2 air voids x 2 NF x 3 temperature x 2 rest periods x 3 replicates). Due to the
167 huge number of tests required, the factorial design was reduced from 432 tests to 288 tests,
168 utilizing a well-known design optimizing criteria named D-optimality.

169 Furthermore, at a later stage of the project, due to the need to check the relationship
170 between the endurance limit, rest period, and strain level, an additional study was performed.
171 This study introduced two new rest periods (5 and 10 sec.), and one new strain level (M level) to
172 the previously used experiment conditions with a total number of 180 new tests.

173 Due to the extensive duration of the test, it was decided to run all tests with rest periods
174 up to 20,000 cycles only. Extrapolation were utilized to find the values of SR for the tests with
175 rest period at the number of cycles bigger than 20,000. The primary measurable variable for each
176 test was the stiffness ratio (SR) at the end of the loading cycles.

177 **5. Model Generation Utilizing Artificial Neural Network**

178 **5.1 Background**

179 Neural networks are highly interconnected networks that have a very strong computational and
180 pattern recognition capabilities. The strength of those networks is in the simulation of the brain
181 working mechanism (Kustrin et al 2000). Figure 3 demonstrates the similarity between nerve
182 neuron cell and an artificial neuron in a network.

183 Ceylan (2014) indicated that “neural networks are information processing computational
184 tools in which highly interconnected neurals work in harmony to solve complex problems in a
185 nontraditional manner. This power of NNs, emulating the biological nerves system, lies in the
186 tremendous numbers of interconnections”. The study concluded that there is a growing usage of
187 the ANN in the engineering filed for traditional numerical and statistical methods such as

188 regression analysis. The grown usage is due to its ability to provide engineers with a
189 sophisticated real-time analysis and results without the need for complex analysis procedures for
190 the input values nor to a large computational power similar to other analysis methods such as
191 finite element solution techniques.

192 **5.2 Utilized Model Architecture**

193 A three-layer feed-forward backpropagation neural network with a sigmoid activation function
194 and one hidden layer are the most common types of neural networks. Also, one hidden layer is
195 typically sufficient for solving most of the non-linear problems without network overfitting
196 (Chan and Chan 2016). For the purpose of this study, a three-layer feed-forward neural network,
197 with a backpropagation-error calculation algorithm and two neurons in the hidden layer, was
198 utilized.

199 Figure 4 demonstrates the utilized network architecture for the study, and its main
200 components may be summarized as follows:

- 201 1) Input layer (i) with four input neurons, one neuron for each independent variable.
202 2) Weight factors (W_{ih}) between the input layer (i) and the hidden layer (h). The weight
203 matrix contained eight different values, one value from each input to each neuron.
204 3) Hidden layer (h) with two hidden neurons having a tan-sigmoid activation function and
205 two biases values (b_{h1} and b_{h2}).
206 4) Weight factors (W'_{ho}) between the hidden layer and the output layer. The weight matrix
207 contained two values, one value from each hidden neuron to the output neuron.
208 5) Output layer (o) with one output neuron for the dependent variable having a linear
209 transfer function and single bias value (B_o).

210 **5.3 Model Training Methodology and Evaluation**

211 Beam fatigue test data set as extracted from NCHRP project 944-A described above contained
212 five different variables: 1) The stiffness ratio at cycle number, 2) Initial stiffness, 3) Rest period,
213 4) Cycles number, and 5) The applied strain. The model was developed and trained to predict the
214 applied strain as a function of the stiffness ratio at cycle number, initial stiffness, rest period, and
215 cycles number as shown in Equation 1.

$$216 \quad \text{Applied Strain} = f(\text{Initial Stiffness, Rest Period, Stiffness Ratio, Cycles Number}) \quad (1)$$

217 The developed model was trained utilizing the extracted 934 data points in MATLAB
218 (MATLAB R2015a, The Math Works Inc.) by feeding the logarithm of initial stiffness, tan
219 hyperbolic of the rest period, stiffness ratio, and the logarithm of number of cycles to failure in
220 the input layer. In addition, the logarithm value of the applied strain was assigned to the output
221 layer. The training was conducted utilizing Levenberg-Marquardt backpropagation algorithm in
222 MATLAB (MATLAB R2015a, The Math Works Inc.). This training algorithm divides the
223 training data into three categories. The first 70% of the data was utilized for training the model,
224 while the remaining 30% of the data was divided into model testing and validation data sets. As
225 shown in Figure 5, as an effort to avoid overfitting and maintain network generalization, the

226 training was stopped when the validation data set error had stopped decreasing (Elbagalati et al.
227 2017).

228 The model performance was evaluated by MATLAB as shown in Figure 6 internally and
229 externally by utilizing Analysis of Variance (ANOVA) in Excel as shown in Table 1. Figure 6
230 demonstrates the ability of the model in the prediction of the strain for all data sets with a
231 coefficient of determination (R^2) value of 0.93, indicating a high model reliability. In addition, as
232 shown within Table 1, the model has a significance F-value of 0 and reasonable value of 32.54 as
233 a standard error; therefore, this model is statistically valid.

234 **5.4 Rule Extraction from the Generated ANN Model - ANN Equation**

235 Despite the fact that ANN is a reliable tool for analysis and data classification, many of the
236 researchers considered it as a black box due to their inability to have a clear understanding for
237 what is happening inside the model.

238 Recently, researchers had attempted to open this black box and generate rules from the
239 results of the trained ANN models (Augasta and Kathirvalavakumar 2012; Chan and Chan
240 2016). There are three main approaches for ANN rule extraction as follows: 1) decompositional,
241 2) Pedagogical, and 3) Eclectic. Decompositional is referring to when the network weights, bias,
242 and activation function values are utilized to extract the rule. Pedagogical is when the
243 relationship between the input and output of the trained ANN network is studied to generate a
244 rule that has the ability to replicate the results of the trained ANN network without the need of
245 the exploration of the ANN network structure. Finally, eclectic, which is considered as a hybrid
246 approach of the two previous approaches, is when the relationship between the input and output
247 as well as the weights and bias values for the trained ANN network are utilized for rule

248 extraction (Augasta and Kathirvalavakumar 2012; Chan and Chan 2016). For the purpose of rule
 249 extraction in this paper, the eclectic approach was utilized.

250 From the utilized ANN structure, as shown in Figure 4, it can be concluded that the
 251 weights from the input layer to the hidden layer, the bias values in the hidden layer, the weights
 252 from the hidden layer to the output layer, and the bias values in the output layer are needed to
 253 extract the rule form the trained ANN network. The values of the weights and biases are
 254 emphasized below as extracted from MATLAB (MATLAB R2015a, The Math Works Inc.).

$$255 \mathbf{W}_{ih} = \begin{bmatrix} -1.1609 & 0.3925 & 0.0476 & -0.3193 \\ 0.1329 & 0.0318 & 0.0318 & -0.2113 \end{bmatrix} \quad \mathbf{W}'_{ho} = \begin{bmatrix} -0.9741 \\ -0.5039 \end{bmatrix}$$

$$256 \mathbf{b}_{hi} = \begin{bmatrix} 1.9361 \\ 0.0575 \end{bmatrix} \quad \mathbf{B}_o = [2.5883]$$

257 The extracted weights, the network structure, and the relationship between the input and
 258 the output of the ANN network were utilized, along with statistical analysis techniques to extract
 259 the rule and generate a stand-alone equation from the trained ANN model. The extracted
 260 equation was as shown in Equation 2.

$$261 \quad \mathcal{E} = 10^{(-0.28256 \text{Log}(E_o) + 0.1058 \tanh(RP) - 0.06934 \text{Log}(N_f) - 0.11089(SR) + 3.40365)} \quad (2)$$

262 where,

263 ε = applied strain (microstrain)

264 E_o = initial stiffness (ksi)

265 RP = rest period (seconds)

266 N_f = number of cycles to failure

267 SR = stiffness ratio

268 The generated stand-alone equation was tested utilizing all of the modeling data (934 data
 269 sets) and it was found to have an acceptable coefficient of determination (R^2) value of 0.74 as

270 shown in Figure 7. In addition, the statistical analysis results for the developed equation as
 271 shown in Table 2 clearly demonstrates that it is statistically valid since that the model has a
 272 significance F-value much lower than 0.05.

273 **5.5 Simplified ANN Endurance Limit Stand-Alone Equation**

274 The extracted equation as well as the generated ANN model may be utilized to calculate the
 275 endurance limit value for the HMA by the interpretation of endurance limit definition into
 276 numbers. As discussed under the literature review part, the endurance limit is the strain level at
 277 which no damage accumulation will occur in the HMA layer. Simply, this strain level maybe
 278 calculated by substituting a stiffness ratio value of 1 and number of cycles to failure of 20,000 in
 279 the equation or the developed ANN model. In other words, the calculated strain value when the
 280 final stiffness is equal to the initial stiffness is the endurance limit.

281 Equation 3 was generated by substituting a stiffness ratio value of 1 and the numbers of cycles to
 282 failure value of 20,000 in Equation 2 to calculate the endurance limit directly for different initial
 283 stiffness and rest period values.

284

$$285 \quad EL = 10^{(-0.28256 \text{Log}(E_o) + 0.1058 \tanh(RP) + 2.99452658)} \quad (3)$$

286 where,

287 EL = endurance limit strain (microstrain)

288 E_o = initial flexural stiffness (ksi)

289 RP = rest period (seconds), \neq zero

290 The ability of this equation to replicate the value of endurance limit as predicted by the
 291 generated ANN model was graphically evaluated as shown in Figure 8 and found to have a high
 292 coefficient of determination (R^2) value of 0.98. Having this high coefficient of determination

293 (R^2) value clearly demonstrates that the equation has a great ability to replicate the endurance
 294 limit values as calculated by the ANN model and may be utilized for endurance limit
 295 calculations.

296 **5.6 Endurance Limit Values Comparison**

297 The EL values as calculated utilizing the stand-alone equation were compared to the EL values
 298 as calculated utilizing the NCHRP 944-A generated equation:

$$\begin{aligned}
 299 \quad SR = & 2.0844 - 0.1386 \times \log(E_o) - 0.4846 \times \log(\epsilon) - 0.2012 \times \log(N) + 1.4103 \times \\
 300 \quad & \tanh(0.8471 \times RP) + 0.0320 \times \log(E_o) \times \log(\epsilon) - 0.0954 \times \log(E_o) \times \tanh(0.7154 \times \\
 301 \quad & RP) - 0.4746 \times \log(\epsilon) \times \tanh(0.6574 \times RP) + 0.0041 \times \log(N) \times \log(E_o) + 0.0557 \times \\
 302 \quad & \log(N) \times \log(\epsilon) + 0.0689 \times \log(N) \times \tanh(0.259 \times RP) \qquad (4)
 \end{aligned}$$

303 where,

304 ϵ = strain (microstrain)

305 E_o = initial flexural stiffness (ksi)

306 RP = rest period (seconds)

307 N = number of cycles

308 The EL values were calculated as the strain values when the stiffness ratio is 1 and the
 309 number of cycles to failure is 20,000 cycles utilizing equation 4. However, strain values related
 310 to zero rest period tests were excluded from the comparison since that when the rest period is
 311 zero there will be no healing for the asphalt; therefore, there will be no EL strain values.

312 Good correlation between both EL values was found with a coefficient of determination
 313 (R^2) value of 0.8 as shown in Figure 9. However, there are considerable differences between both
 314 values, which is demonstrated by Figure 9 and Table 3, which shows the standard error value.

315 In this comparison, there are some important points to consider, such as what was done is
 316 comparing predicted to predicted values. All the compared values were predicted values, not

317 measured. Second, in the NCHRP 944-A project, no beam was tested on its endurance limit;
318 therefore, there is no measured value of the EL strain. Third, when predicting the EL value
319 utilizing the strain model developed under the NCHRP 944-A project, the relationship line
320 between the stiffness ratio and the strain was extended linearly until reaching a SR of 1. In other
321 words, a linear relationship (on the log scale) between the strain and the SR was assumed
322 without having any data point in this area as shown in Figure 10. In fact, the newly developed
323 Artificial Neural Network Model (ANN) maybe stronger in prediction when it comes to this
324 point since that it drives the relationship between the data based on the nature and correlation
325 existed within it, in a way to simulate the brain working mechanism.

326 The newly developed ANN model had a higher value of the coefficient of determination
327 (R^2) when compared to the model developed under the NCHRP project 944-A, and that gives an
328 indication about the ability of the model in the strain prediction, thus; it may be used for EL
329 strain prediction.

330

331

332 **6. Summary and Conclusions**

333 The asphalt healing is directly related to the endurance limit; therefore, the endurance limit is not
334 a single value. The importance of the endurance limit is in the design of the perpetual pavements,
335 since that, if a pavement layer is experiencing a tensile strain equivalent to the endurance limit
336 stain or lower, no damage will accumulate in the pavement layer and it will never fail under
337 repeated loading cycles due to fatigue cracking.

338 This paper aimed to utilize ANN modeling to create a prediction model for the endurance
339 limit and extract the rule (stand-alone equation) from it. The developed model was generated
340 utilizing 934 beam fatigue test data points as extracted from NCHRP project 944-A and had a

341 good prediction accuracy with a coefficient of determination value (R^2) value of 0.93. Eclectic
342 extraction approach was utilized along with statistical analysis techniques to extract the rule from
343 the generated ANN model and create a stand-alone equation that maybe utilized outside the
344 MATLAB model environment. The extracted stand-alone equation had a reasonable prediction
345 accuracy with a coefficient of determination value (R^2) value of 0.74. In addition, the ANN
346 model utilized architecture as well as the training techniques, utilized activation, and transfer
347 functions were discussed in detail to provide a clear procedure that maybe utilized to model any
348 other specific beam fatigue test data and create an ANN prediction model.

349 The developed simplified endurance limit equation (Equation 3) was able to replicate the
350 ANN model calculated endurance limit values with a high coefficient of determination value
351 (R^2) value of 0.97. Having the coefficient of determination value (R^2) value indicates the
352 reliability of the endurance limit derived equation and envision its high ability to simulate the
353 endurance limit calculation utilizing the ANN model in MATLAB environment.

354 The EL values as calculated utilizing the stand-alone equation were compared to the EL
355 values as calculated utilizing the NCHRP 944-A generated equation. Both EL values founded to
356 be well correlated with a coefficient of determination value (R^2) of 0.8. However, there are
357 considerable differences between both EL predicted values. The differences in the predicted
358 values of the EL strain maybe due the nonlinearity of the relationships created within the ANN
359 model to simulate the brain working mechanism. The strength of those relationships is that they
360 were created for the given input output data (custom made based on the nature of the data);
361 therefore, the ANN model is stronger in the prediction when compared to the regular regression
362 models presented under the NCHRP 944-A project.

363 Further testing is required to create a new ANN predicting model and equations for non-
364 conventional asphalt mixtures. In addition, further field verification utilizing an actual pavement
365 section for the developed model as well as the equation is highly recommended.

366 7. References

367 Abojaradeh, M. 2003. Predictive fatigue models for Arizona asphalt concrete mixtures.
368 Doctoral dissertation, Arizona State University.

369 Agatonovic-Kustrin, S. and Beresford, R. 2000. Basic concepts of artificial neural network
370 (ANN) modeling and its application in pharmaceutical research. *Journal of*
371 *pharmaceutical and biomedical analysis*, 22(5), pp.717-727.

372 Augasta, M.G. and Kathirvalavakumar, T. 2012, March. Rule extraction from neural
373 networks—A comparative study. In *Pattern Recognition, Informatics and Medical*
374 *Engineering (PRIME)*, 2012 International Conference on (pp. 404-408). IEEE.

375 Carpenter, S.H. 2006. Fatigue performance of IDOT mixtures, *Civil Engineering Studies*.
376 Illinois Center for Transportation Series No 07.-007. University of Illinois at Urbana-
377 Champaign.

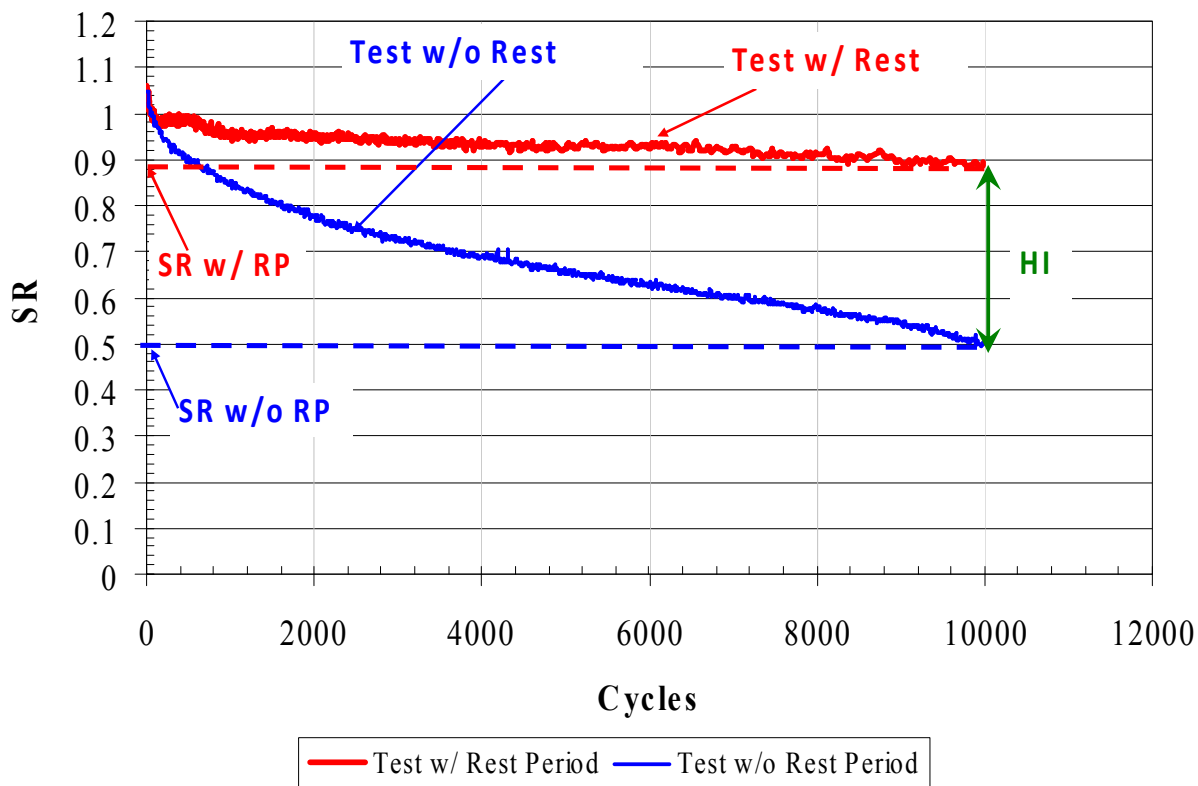
378 Castro, M. and Sánchez, J.A. 2006. Fatigue and healing of asphalt mixtures: discriminate
379 analysis of fatigue curves. *Journal of transportation engineering*, 132(2), pp. 168-174.

380 Ceylan, H., Bayrak, M.B. and Gopalakrishnan, K. 2014. Neural networks applications in
381 pavement engineering: A recent survey. *International Journal of Pavement Research and*
382 *Technology*, 7(6), pp.434-444.

383 Chan, V. and Chan, C.W. 2016, August. Development and application of an algorithm for
384 extracting multiple linear regression equations from artificial neural networks for

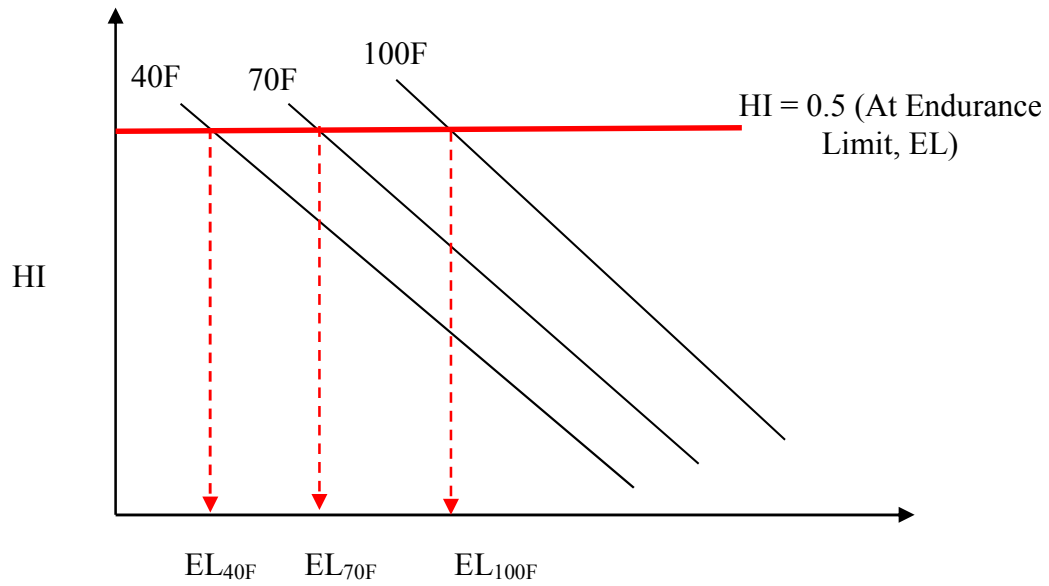
- 385 nonlinear regression problems. In *Cognitive Informatics & Cognitive Computing (ICCI**
386 *CC)*, 2016 IEEE 15th International Conference on (pp. 479-488). IEEE.
- 387 Elbagalati, O., Elseifi, M. A., Gaspard, K., & Zhang, Z. 2017. Development of an artificial
388 neural network model to predict subgrade resilient modulus from continuous deflection
389 testing. *Canadian Journal of Civil Engineering*, 44(9), 700-706.
- 390 Lytton, R. 2000. Characterizing asphalt pavements for performance. *Transportation Research*
391 *Record: Journal of the Transportation Research Board*, (1723), pp.5-16.
- 392 Maupin Jr, G.W. and Freeman Jr, J.R. 1976. Simple procedure for fatigue characterization of
393 bituminous concrete (No. FHWA-RD-76-102 Final Rpt.).
- 394 Mc Elvaney, J. and Pell, P.S. 1973. Fatigue damage of asphalt. Effect of rest periods.
395 *Highways and Road Construction*, 41(1766).
- 396 Miller, J.S. and Bellinger, W.Y. 2003. Distress identification manual for the long-term
397 pavement performance program. Publication no. FHWA-Rd-03-031, Strategic Highway
398 Research Program, National Research Council. Washington, DC.
- 399 Monismith, C. L., and D. B. McLean. 1972. Structural design considerations. *Proceedings of*
400 *the Association of Asphalt Paving Technologists*, Vol. 41.
- 401 Monismith, C.L. and J.A. Deacon. 1969. Fatigue of asphalt paving mixtures. *Journal of*
402 *Transportation Engineering*, 95(2): pp. 317-345.
- 403 NCHRP Project 944-A. 2010. Validating an endurance limit for HMA pavements:
404 Laboratory experiment and algorithm development. Quarterly progress report, Arizona
405 State University, Tempe, Arizona.

- 406 Newcomb, D.E., Buncher, M. and Huddleston, I.J. 2001. Concepts of perpetual pavements.
407 Transportation Research Circular, 503, pp. 4-11.
- 408 Peterson J.C. 1984. Chemical composition of asphalt related to asphalt durability: State of the
409 art, Transportation Research Record, Vol #999.
- 410 Prowell, B., Brown, E., Anderson, R., Daniel, Jo., Swamy, A., Von Quintus, H., Shen, S.,
411 Carpenter, S., Bhattacharjee, S., Maghsoodloo, S. 2010. Validating the fatigue endurance
412 limit for hot mix asphalt. NCHRP Report 646.
- 413 Setiono, R., Leow, W. K., & Zurada, J. M. 2002. Extraction of rules from artificial neural
414 networks for nonlinear regression. IEEE Transactions on Neural Networks, 13(3), 564-
415 577.
- 416 Souliman, M. 2012. Integrated predictive model for healing and fatigue endurance limit for
417 asphalt concrete. Ph.D. Dissertation, Arizona State University, Tempe, AZ.
- 418 Suresh, S., 1998. Fatigue of materials. 2nd Edition. Cambridge University Press, USA, pp 1-
419 679
- 420 Thompson M. R., Carpenter S. H. 2006. Considering hot-mix-asphalt fatigue endurance limit
421 in full-depth mechanistic-empirical pavement design. International conference on
422 perpetual pavement, Ohio.
- 423 Willis, J., Timm, D. 2009. Field-based strain thresholds for flexible perpetual pavement
424 design. national center for asphalt technology. NCAT Report 09-09.
- 425 Wöhler, A. 1860. Versuche uber die festigkeit der eisenbahnwagenachsen. English summary
426 (1867). Engineering, 4, 160-161.
- 427



428
429
430

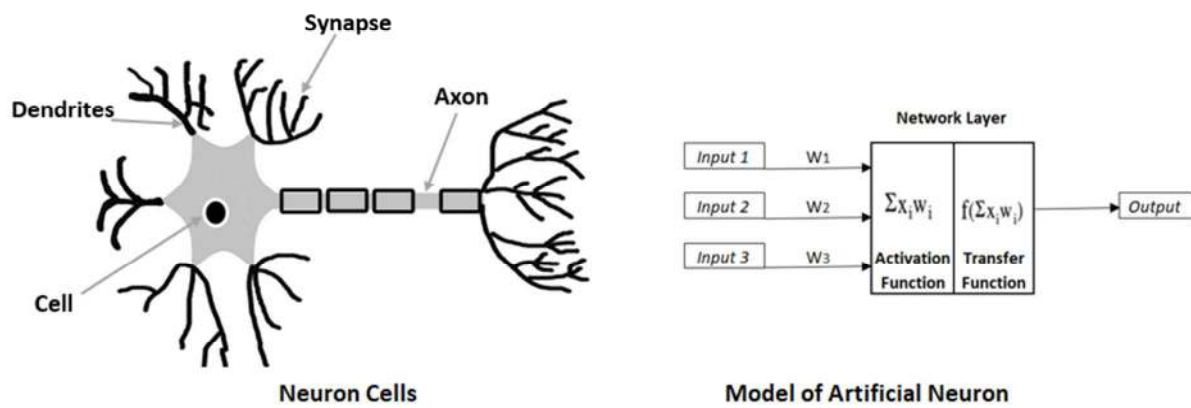
Figure 1. Healing index definition (Souliman 2012)



431
432
433
434
435

Figure 2. Endurance limit determination at each temperature based on HI (Souliman 2012)

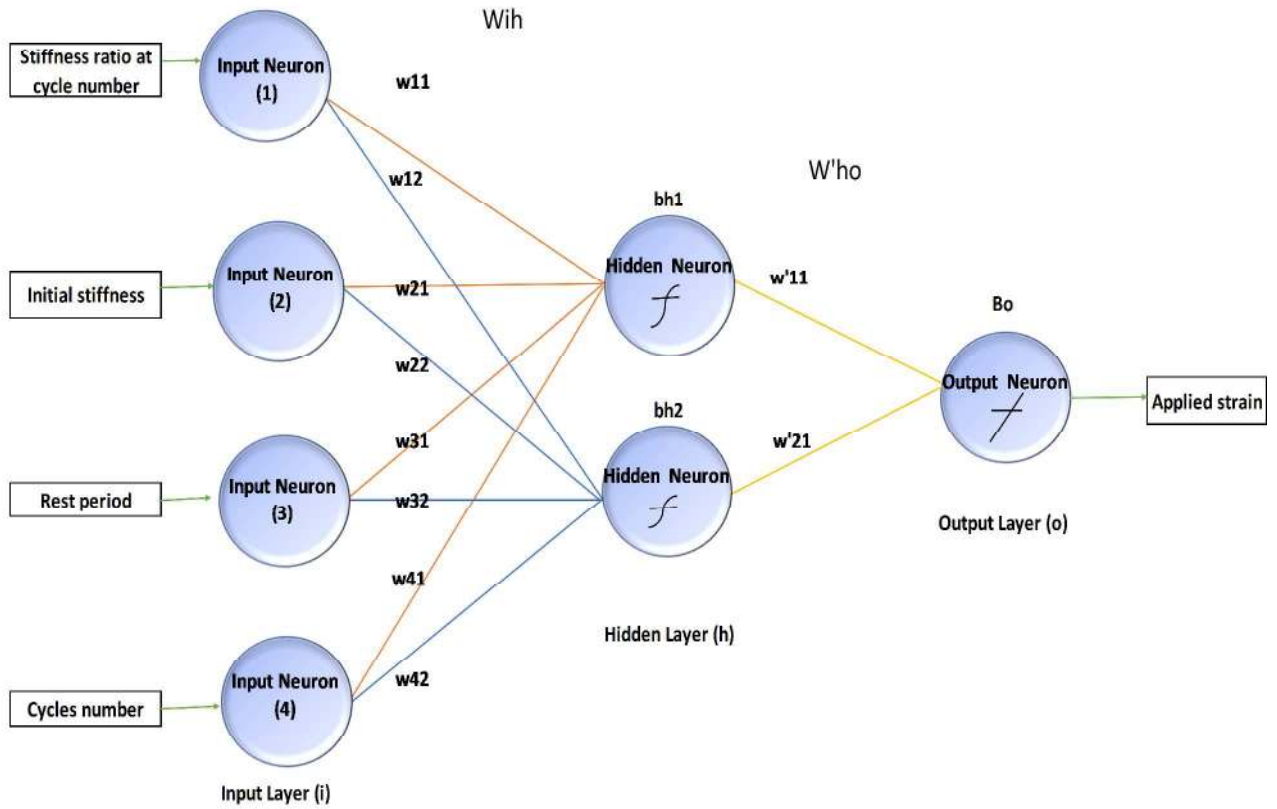
Draft



436
437
438

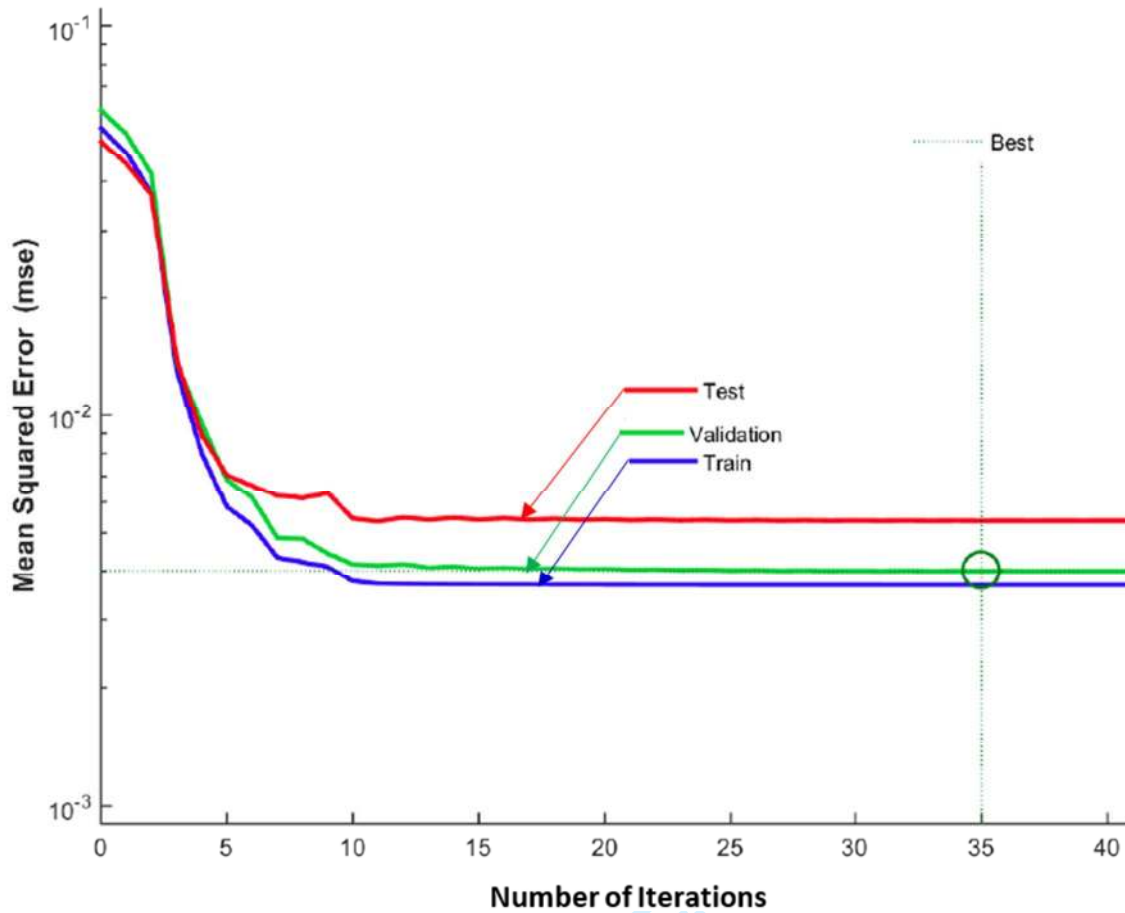
Figure 3. Similarity between nerve neuron cell and an artificial neuron

Draft



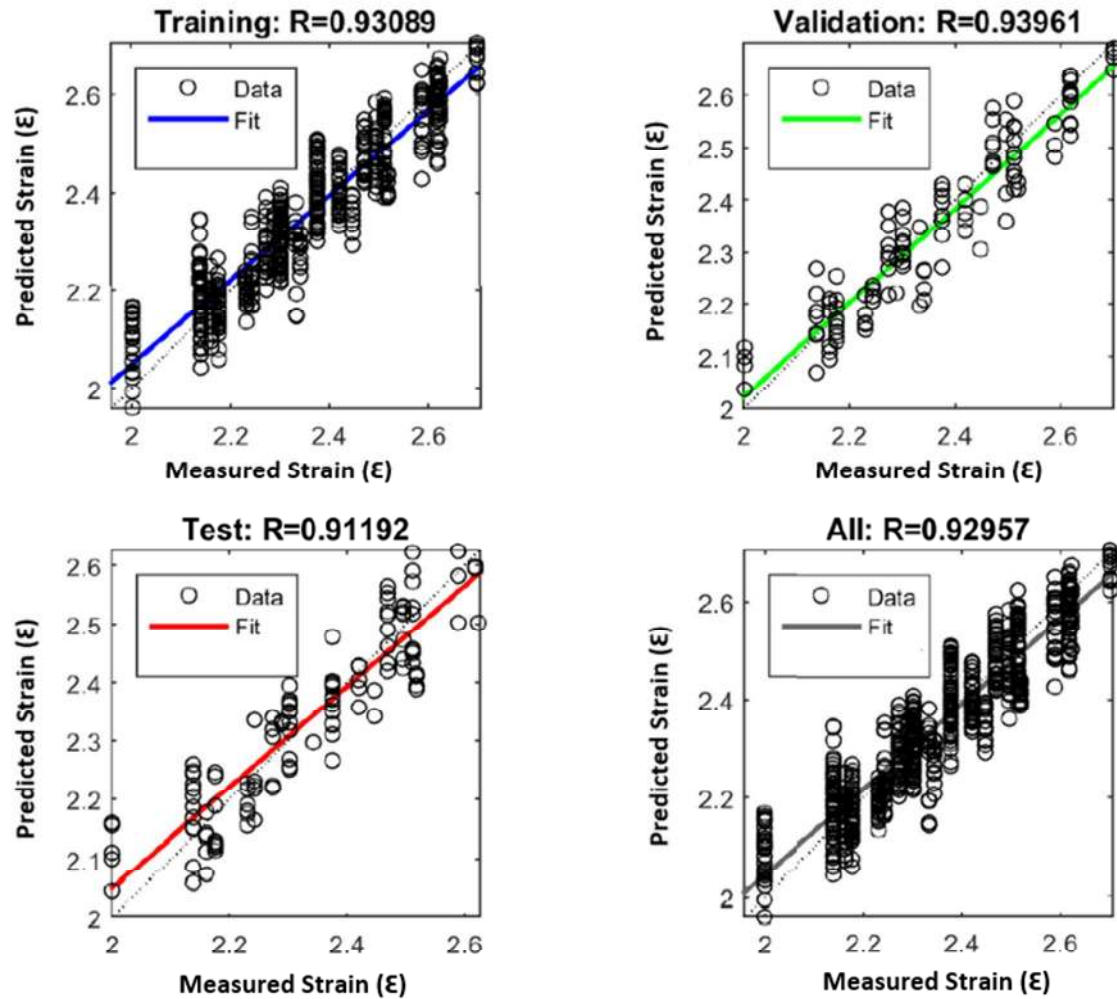
439
440
441

Figure 4. ANN utilized model architecture



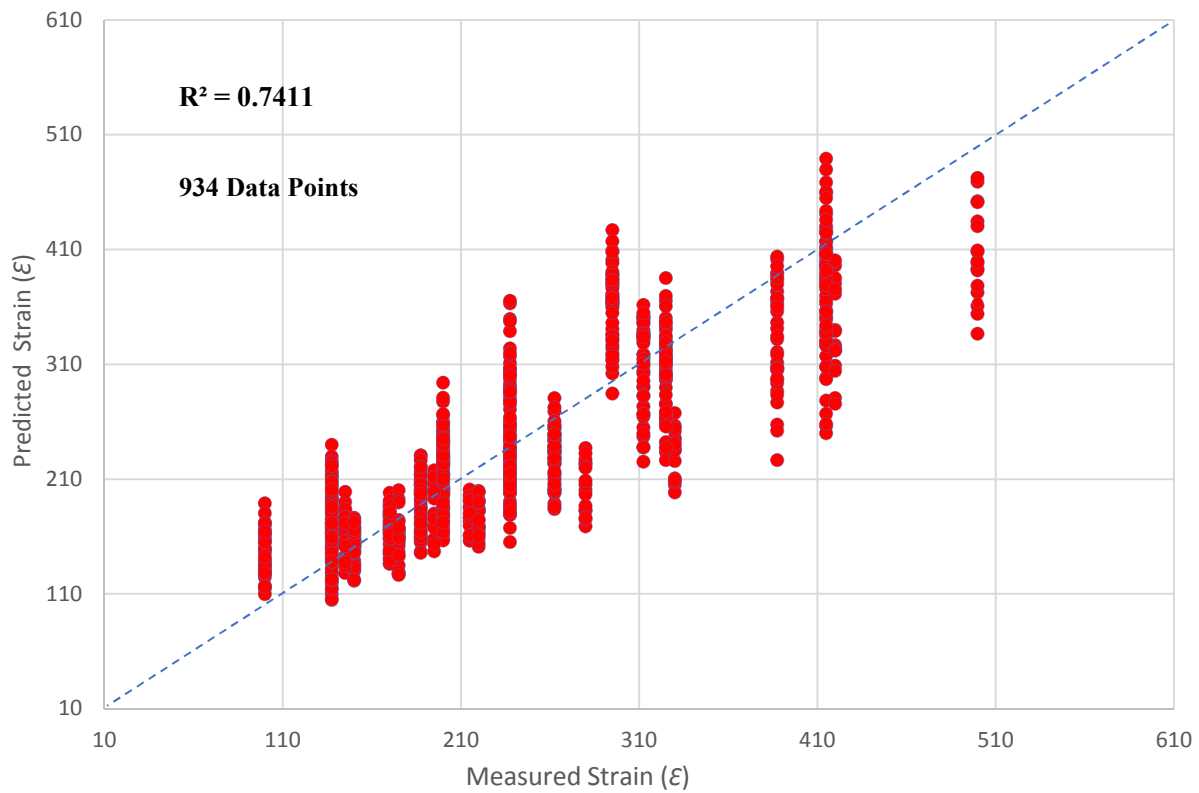
442
443
444
445

Figure 5. Number of iterations/ epochs required for model training (MATLAB R2015a, The Math Works Inc.)



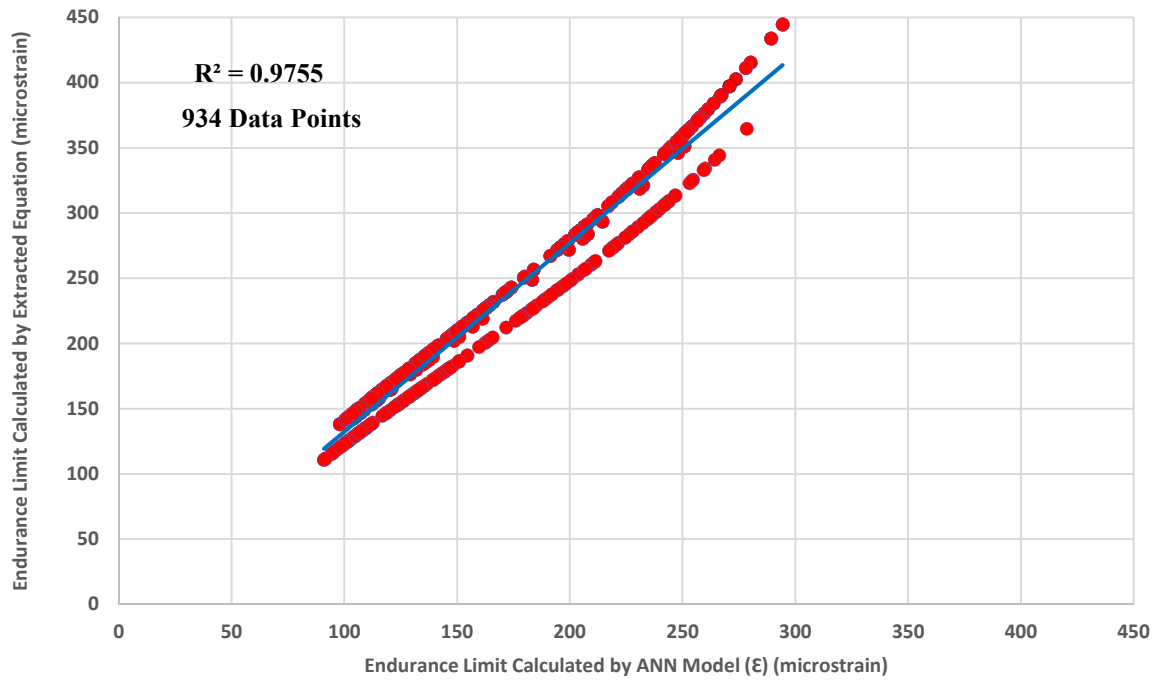
446
447
448
449
450

Figure 6. Regression plots for training, validation, testing, and overall data (MATLAB R2015a, The Math Works Inc.)



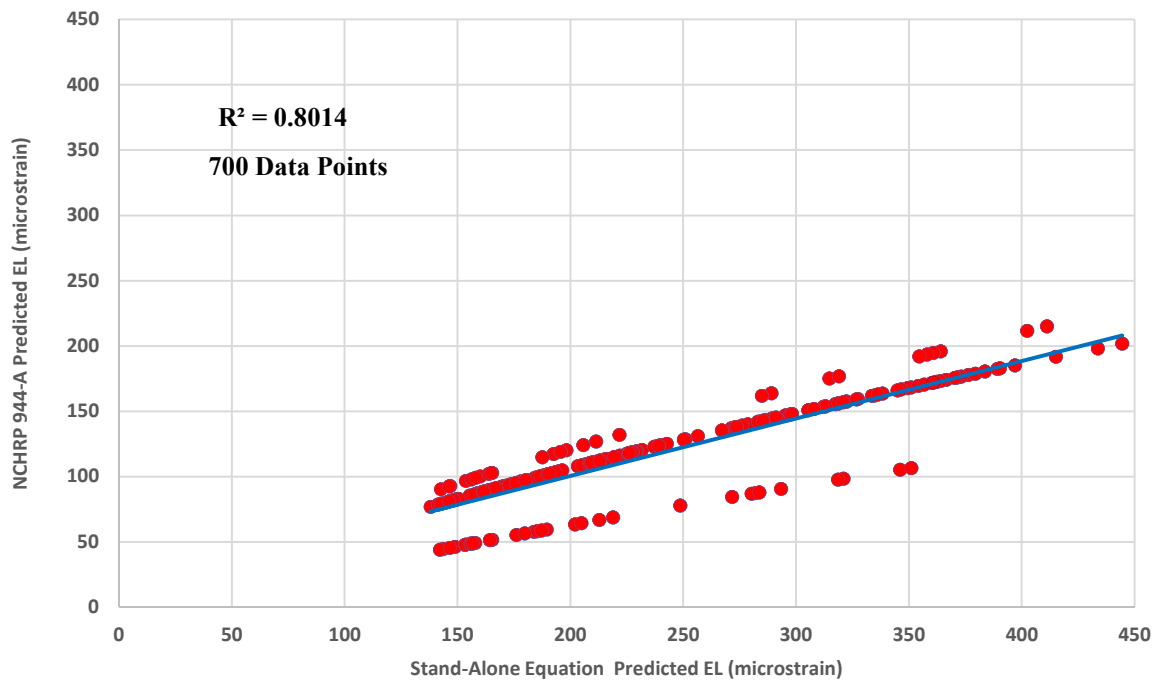
451
452
453
454

Figure 7. Predicted VS measured values of strain for 934 data sets utilizing the generated ANN equation (Equation 2).



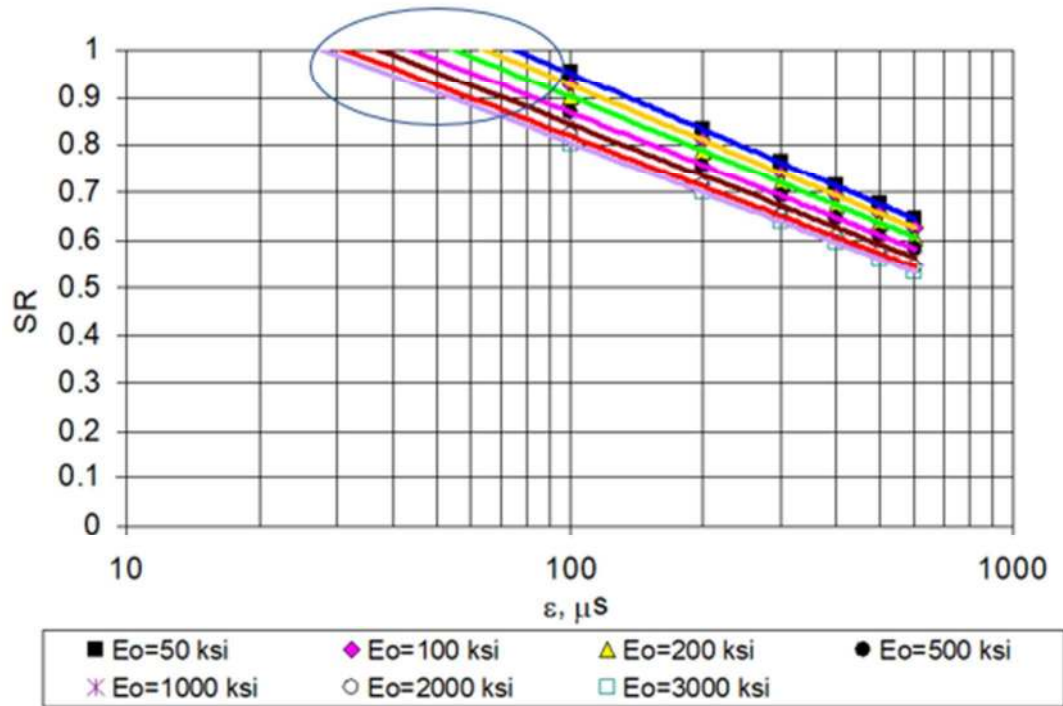
455
456
457
458

Figure 8. Endurance limit values calculated utilizing the ANN model VS simplified Equation (3) calculated values.



459
460
461
462

Figure 9. Endurance limit values calculated utilizing the simplified Equation (3) vs NCHRP 944-A generated equation values.



463
464
465
466
467

Figure 10. SR vs strain for several initial stiffness values and 1 second rest period. (Souliman 2012)

468 **Table 1. Analysis of variance for predicted VS measured values of strain for 934**
 469 **data sets utilizing the developed ANN model.**

470

SUMMARY OUTPUT

<i>Regression Statistics</i>					
Multiple R		0.932172173			
R Square		0.868944959			
Adjusted R Square		0.868804342			
Standard Error		32.53500727			
Observations		934			

ANOVA					
	<i>df</i>	<i>SS</i>	<i>MS</i>	<i>F</i>	<i>Significance F</i>
Regression	1	6541183	6541183	6179.516	0
Residual	932	986546.9	1058.527		
Total	933	7527729			

471

472

473 **Table 2. Analysis of variance for predicted VS measured values of strain for 934**
 474 **data sets utilizing the generated ANN equation (Equation 2).**
 475

SUMMARY OUTPUT

<i>Regression Statistics</i>					
Multiple R					0.85794261
R Square					0.736065522
Adjusted R Square					0.735782331
Standard Error					0.076153751
Observations					934

ANOVA					
	<i>df</i>	<i>SS</i>	<i>MS</i>	<i>F</i>	<i>Significance F</i>
Regression	1	15.07366	15.07366	2599.179	7.9558E-272
Residual	932	5.405035	0.005799		
Total	933	20.4787			

476
477

478 **Table 3. Analysis of variance for endurance limit values calculated utilizing the**
 479 **simplified Equation (3) vs NCHRP 944-A generated equation values for 700 data**
 480 **sets.**
 481

SUMMARY OUTPUT

<i>Regression Statistics</i>					
Multiple R		0.895184			
R Square		0.801355			
Adjusted R Square		0.80107			
Standard Error		34.74031			
Observations		700			

<i>ANOVA</i>					
	<i>df</i>	<i>SS</i>	<i>MS</i>	<i>F</i>	<i>Significance F</i>
Regression	1	3398362.431	3398362	2815.803	3.6058E-247
Residual	698	842408.578	1206.889		
Total	699	4240771.009			

482

483